Near equilibrium dynamics of nonhomogeneous Kirchhoff filaments in viscous media

A. F. Fonseca[1] and M. A. M. de Aguiar[1,2]

[1]*Instituto de Física ''Gleb Wataghin,'' Universidade Estadual de Campinas, Unicamp 13083-970, Campinas, SP, Brazil*

[2]*Center for Theoretical Physics, Laboratory for Nuclear Science and Department of Physics, Massachusetts Institute of Technology, Cambridge, Massachusetts 02139*

We study the near equilibrium dynamics of nonhomogeneous elastic filaments in viscous media using the Kirchhoff model of rods. Viscosity is incorporated in the model as an external force, which we approximate by the resistance felt by an infinite cylinder immersed in a slowly moving fluid. We use the recently developed method of Goriely and Tabor [Phys. Rev. Lett. **77**, 3537 (1996); Physica D **105**, 20 (1997); **105**, 45 (1997)] to study the dynamics in the vicinity of the simplest equilibrium solution for a closed rod with nonhomogeneous distribution of mass, namely, the planar ring configuration. We show that small variations of the mass density along the rod are sufficient to couple the symmetric modes of the homogeneous rod problem, producing asymmetric deformations that modify substantially the dynamical coiling, even at quite low Reynolds number. The higher-density segments of the rod tend to become more rigid and less coiled. We comment on possible applications to DNA.

I. INTRODUCTION

A rod, or filament, is a tridimensional object with two of its dimensions much smaller than the third, i.e., with its length much larger than its cross section. The study of the mechanical properties of rods is of interest in many fields of science. Examples are the motion of vortex tubes in hydrodynamics [3] and the shapes and dynamics of biomolecules [4–6] and bacterial fibers [7,8]. In engineering, the theory of rods has been applied to the study of suboceanic cables [9–11] and has lead to important applications in the installation process and stability of optical fibers [12,13].

The dynamics of inextensible rods is governed by the Kirchhoff equations. These equations, to be described in detail in Sec. II, form a set of nine partial differential equations in the time and arclength of the rod, involving the force, torque, and a triad of vectors describing the rod itself. These equations are the result of Newton's second law for the linear and angular momentum applied to the thin body plus a linear constitutive relation between torque and twist. The Kirchhoff model holds true in the approximation of small curvatures of the rod, as compared to the radius of the local cross section.

In most of the cases found in the literature, thin elastic structures are modeled by uniform filaments. In some problems, however, it is important to take into account the nonuniformities of the structure, like its mass density or its bending and twisting stiffness. Going down to microscopic details, some authors [14–16] have applied the so-called sequence dependent anisotropic bendability models to study local bending of DNA. In these models, the rod is divided into small disks, each corresponding to a DNA base pair. The mechanical properties of the disks are assigned according to the base pair it is supposed to represent. This procedure, however, is computationally applicable only to small molecules.

In this paper we give a step towards incorporating fine-structure properties into the continuous rod model [17,1,2]. The main advantage of a continuous treatment of nonunifor-

mities is that they can be included directly into the differential equations describing the dynamics, allowing for the modeling of long nonhomogeneous filaments. In this paper we shall restrict ourselves to the study of *closed* rods whose *mass density* vary periodically, simulating either fine scale properties that have survived the large scale average or the binding of external particles to the filament. More specifically, we study the dynamics of closed rods near their simplest equilibrium configuration, the so-called planar ring solution.

Nonuniformities in the distribution of mass changes the local inertial forces. The effective role of these forces, however, depends crucially on the medium where the rod is immersed. In the case of biomolecules, for instance, inertial forces are not usually considered due to the very small values attained by the Reynolds number in typical biological media. Goldstein and Langer [6] developed a formalism to treat the case where inertial forces are totally discarded. In fact, inertial forces are irrelevant when compared to external forces like gravity or electromagnetic forces if the body is immersed in a very viscous fluid [18]. In this paper, however, we are concerned with internal forces. In particular we wish to answer the question of how a flexible polymer reacts when submitted to a large torsion if its mass distribution is nonuniform. In order to answer this question we generalize the Kirchhoff's equations to model rods immersed in viscous fluids. With these new equations we are able to study the balance between inertial forces, partly due to internal elastic forces, and viscous forces.

The dynamics in the vicinity of a homogeneous planar ring was first studied by Zajac [11], who showed the existence of perturbed solutions for the planar ring with total twist larger than a certain critical value. The Zajac solutions are similar to the (symmetric) normal modes of a string or membrane. In this paper we show that the introduction of small periodic nonhomogeneities into an initially uniform rod may produce important changes in the shape and symmetry of its near equilibrium dynamics, depending on the

periodicity of the perturbation as compared to the linear instability modes (the Zajac modes) of the uniform rod. We also show that, if the total twist of the rod is relatively large, than, even at quite low Reynolds numbers, a nonhomogeneous distribution of mass can change qualitatively the dynamics.

This paper is organized as follow. In Sec. II, we extend the Kirchhoff model to include mass nonuniformities and viscous forces. Nonuniformities in the mass density can be easily included in the Kirchhoff equations, although it complicates the analysis of the near equilibrium dynamics. Viscous forces are incorporated as external forces. These are modeled by the resistance felt by an infinite cylinder in a slowly moving fluid (creeping motion) [19,20]. Nonuniform bending or twisting stiffness can also be introduced in the model, but that will be the subject of a future publication. In Sec. III we describe the famous *twisted planar ring equilibrium solution* of the Kirchhoff equations. In Sec. IV, we apply the method of Goriely and Tabor [2] to study the dynamics in the vicinity of the planar ring configuration for a homogeneous closed rod in a viscous medium. In Sec. V, we consider the nonhomogeneous rod and compare its dynamical evolution with the case of zero viscosity, for the same parameters used in Sec. IV. In Sec. VI, we apply this model to a closed DNA with 168 basepairs. At typical linking number deficit of 5% [21] this closed DNA is stable. But for a total twist deficit (or excess) of the order of 100% the near equilibrium dynamics of the DNA does feel the effects of the mass distribution even at realistic Reynolds numbers. In Sec. VII we summarize our conclusions.

II. KIRCHHOFF MODEL FOR RODS IN A VISCOUS MEDIUM

The Kirchhoff model describes the dynamics of thin elastic filaments within the approximation of linear elasticity theory [17]. The Kirchhoff's equations result from the application of Newton's laws of mechanics to the thin rod, and consist of two equations describing the balance of force and angular momentum, and a third equation containing a constitutive relationship of linear elasticity theory, relating moments to strains.

We introduce the Kirchhoff's model following closely the presentation of Ref. [17]. The classical conservation laws of linear and angular momentum for a tridimensional body of volume V and enclosed area A are

$$\int_A \mathbf{p}_n dS + \int_V \mathbf{f} dV = \int_V \rho \ddot{\mathbf{X}} dV, \qquad (1)$$

$$\int_A (\mathbf{X} \times \mathbf{p}_n) dS + \int_V (\mathbf{X} \times \mathbf{f}) dV = \int_V \rho (\mathbf{X} \times \ddot{\mathbf{X}}) dV. \qquad (2)$$

where $\mathbf{p}_n$ is the contact force per unit area exerted on the oriented surface element $d\mathbf{S} = \mathbf{n} dS$, ρ is the mass density, and $\mathbf{X}$ is the position with respect to a fixed origin. External forces per unit volume acting on the body are represented by the vector $\mathbf{f}$.

We want to apply these equations to the particular case of a rod. For that, we consider the rod as a thin tube whose axis is a smooth curve x in the 3D space parametrized by arclength s, and whose position depends on time: $\mathbf{x} = \mathbf{x}(s,t)$. A *local orthonormal basis*, (or *director basis*) $\mathbf{d}_i = \mathbf{d}_i(s,t)$, $i = 1,2,3$, is defined at each point of the curve, with $\mathbf{d}_3$ chosen as the tangent vector, $\mathbf{d}_3 = \mathbf{x}'$. In this paper we shall use primes to denote differentiation with respect to s and dots to denote differentiation with respect to time. The two orthonormal vectors, $\mathbf{d}_1$ and $\mathbf{d}_2$, lie in the plane normal to $\mathbf{d}_3$, for example along the principal axes of the cross section of the rod. We choose these vectors in such a way that $\mathbf{d}_1, \mathbf{d}_2, \mathbf{d}_3$ form a right-handed orthonormal basis for each value of s and t. The space and time evolution of the director basis along the curve are controlled by *spin* and *twist equations*

$$\mathbf{d}'_i = \mathbf{k} \times \mathbf{d}_i, \qquad \dot{\mathbf{d}}_i = \boldsymbol{\omega} \times \mathbf{d}_i, \qquad i = 1,2,3 \qquad (3)$$

which follow from the orthonormality relations $\mathbf{d}_i \cdot \mathbf{d}_j = \delta_{ij}$. The components of $\mathbf{k}$ and $\boldsymbol{\omega}$ in the director basis are defined as $\mathbf{k} = \Sigma_{i=1}^3 k_i \mathbf{d}_i$ and $\boldsymbol{\omega} = \Sigma_{i=1}^3 \omega_i \mathbf{d}_i$. k_1 and k_2 are the components of the curvature and k_3 is the twist density of the rod. The solution of the spin and twist equations determines $\mathbf{d}_3(s,t)$, which can be integrated to give the space curve $\mathbf{x}(s,t)$. The Kirchhoff model assumes that the filament is thin and weakly bent (i.e., its cross-section radius is much smaller than its length and its curvature at all points). In this approximation it is possible to derive a one-dimensional theory where forces and moments are averaged over the cross sections perpendicular to the central axis (the curve $\mathbf{x}$) of the filament.

Let the material points on the rod be labeled by

$$\mathbf{X}(s,t) = \mathbf{x}(s,t) + \mathbf{r}(s,t), \qquad (4)$$

where

$$\mathbf{r}(s,t) = x_1 \mathbf{d}_1(s,t) + x_2 \mathbf{d}_2(s,t) \qquad (5)$$

gives the position of the point on the cross section $\mathcal{S}$, perpendicular to $\mathbf{x}'$, with respect to the central axis. The total force $\mathbf{F} = \mathbf{F}(s,t)$ and the total moment $\mathbf{M} = \mathbf{M}(s,t)$ on the cross section are defined by

$$\mathbf{F} = \int_{\mathcal{S}(s)} \mathbf{p}_s dS, \qquad (6)$$

$$\mathbf{M} = \int_{\mathcal{S}(s)} \mathbf{r} \times \mathbf{p}_s dS, \qquad (7)$$

where $\mathbf{p}_s$ is the contact force per unit area exerted on the cross section $\mathcal{S}$. In terms of the director basis we write $\mathbf{F} = \Sigma_{i=1}^3 f_i \mathbf{d}_i$ and $\mathbf{M} = \Sigma_{i=1}^3 M_i \mathbf{d}_i$.

In order to derive a set of equations describing the rod as a one-dimensional object, the rod is divided into thin disks of length ds and cross section $S(s)$, and Eqs. (1) and (2) are applied to each of these disks. The result is

$$\mathbf{F}' + \int_{\mathcal{S}(s)} \mathbf{f} \, dS = \int_{\mathcal{S}(s)} \rho \ddot{\mathbf{X}} \, dS, \tag{8}$$

$$\mathbf{M}' + \mathbf{x}' \times \mathbf{F} + \int_{\mathcal{S}(s)} \mathbf{r} \times \mathbf{f} \, dS = \int_{\mathcal{S}(s)} \rho \mathbf{r} \times \ddot{\mathbf{X}} \, dS, \tag{9}$$

where we have written $dV = ds \, dS$ and used the fact that $\mathbf{p}_n$ is nonzero only at the sections $\mathcal{S}(s)$ and $\mathcal{S}(s+ds)$.

In this article we are interested in the dynamics of rods immersed in viscous fluids. We therefore incorporate the viscous friction through the external force f. Assuming that the rod moves slowly in the fluid we approximate the resistance felt by the rod by that felt by an infinite cylinder in a viscous fluid flow. This is a well known result [19,20] and gives the resistance force per unit length in the direction of the flow as

$$f_v = \frac{-4\pi\eta}{0.5 - c - \ln(Ua\rho_m/4\eta)} U, \tag{10}$$

where η is the viscosity of the medium, a is the radius of the cylinder, ρ_m is the density of the medium, U is the velocity of the fluid with respect to the cylinder, and c is the Euler's number. The ratio

$$\frac{Ua\rho_m}{\eta} \tag{11}$$

is the Reynolds number R_e of the system.

Since viscous forces act only on the external surface of the rod, we impose that the total external force integrated on the volume to be the same as the force per unit length integrated on ds, i.e., $\int_V \mathbf{f} \, dV = \int_L \mathbf{f}_v \, ds$. We find that the external force in Eqs. (8) and (9) has to be written as

$$\mathbf{f} = \mathbf{f}_v \frac{\delta(r-a)}{2\pi r}. \tag{12}$$

Using Eqs. (4) and (5) and assuming that the rod has a uniform circular cross section of area A, Eqs. (8) and (9) can be simplified to yield:

$$\mathbf{F}'' - bA\dot{\mathbf{d}}_3 = \frac{\rho'(s)}{\rho(s)} (\mathbf{F}' - bA\dot{\mathbf{x}}) + \rho(s)A\ddot{\mathbf{d}}_3, \tag{13}$$

$$\mathbf{M}' + \mathbf{d}_3 \times \mathbf{F} - 2bI(\mathbf{d}_1 \times \dot{\mathbf{d}}_1 + \mathbf{d}_2 \times \dot{\mathbf{d}}_2)$$
$$= \rho(s)I(\mathbf{d}_1 \times \ddot{\mathbf{d}}_1 + \mathbf{d}_2 \times \ddot{\mathbf{d}}_2), \tag{14}$$

where I is the principal moment of inertia of the cross section and b is obtained from Eq. (10):

$$b = \frac{1}{A} \left(\frac{4\pi\eta}{0.5 - c - \ln(R_e/4)} \right). \tag{15}$$

Notice that Eq. (8) was differentiated with respect to s. In the case of constant mass density, $\rho' = 0$, this has the effect of removing $\mathbf{x}$ from the system of equations, leaving only the director basis vectors as variables. To get rid of the $\dot{\mathbf{x}}$ in the

term with ρ', one has to differentiate this equation once more. We shall get back to this point later on.

In order to close the system of equations we need a *constitutive relation* relating the local forces and moments (stresses) to the elastic deformations of the body (strains). In linear theory of elasticity, for a homogeneous elastic material, the stress is proportional to the deformation if this deformation is small. The Young's modulus (E) and the Shear modulus (μ) characterize the elastic properties of the material. Therefore, it is possible to obtain, for small deformation, a constitutive relation for the moment. In the director basis the relation is [17]

$$\mathbf{M} = EI(k_1 - k_1^u)\mathbf{d}_1 + EI(k_2 - k_2^u)\mathbf{d}_2 + 2\mu I(k_3 - k_3^u)\mathbf{d}_3, \tag{16}$$

where k_i are the components of the twist vector and k_i^u are the components of the twist vector in the unstressed configuration. The case $k_i^u = 0$ corresponds to the case of a naturally straight and untwisted rod. We shall assume $k_i^u = 0$.

Equations. (13), (14) and (16) can be further simplified by the introduction of scaled variables. We first write the mass density in the form

$$\rho = \rho_0(1 + \delta\rho), \tag{17}$$

where ρ_0 is constant and $\delta\rho$ carries the fluctuations of ρ along the rod. Following Ref. [1] we make the changes:

$$t \to t\sqrt{\frac{I\rho_0}{AE}}, \quad s \to s\sqrt{\frac{I}{A}}, \quad \mathbf{F} \to AE\mathbf{F}, \quad b \to \sqrt{\frac{AE\rho_0}{I}}b, \tag{18}$$

$$\mathbf{M} \to \mathbf{M}E\sqrt{AI}, \quad \kappa \to \kappa\sqrt{\frac{A}{I}}, \quad \boldsymbol{\omega} \to \boldsymbol{\omega}\sqrt{\frac{AE}{I\rho_0}}, \quad \rho \to \rho/\rho_0.$$

In the new variables the Kirchhoff equations become

$$\mathbf{F}'' - b\dot{\mathbf{d}}_3 = \frac{\rho'(s)}{\rho(s)} (\mathbf{F}' - b\dot{\mathbf{x}}) + \rho(s)\ddot{\mathbf{d}}_3, \tag{19}$$

$$\mathbf{M}' + \mathbf{d}_3 \times \mathbf{F} - 2b(\mathbf{d}_1 \times \dot{\mathbf{d}}_1 + \mathbf{d}_2 \times \dot{\mathbf{d}}_2)$$
$$= \rho(s)(\mathbf{d}_1 \times \ddot{\mathbf{d}}_1 + \mathbf{d}_2 \times \ddot{\mathbf{d}}_2), \tag{20}$$

$$\mathbf{M} = k_1\mathbf{d}_1 + k_2\mathbf{d}_2 + \Gamma k_3\mathbf{d}_3, \tag{21}$$

where $\rho = 1 + \delta\rho$ is now a dimensionless function of arclength s and $\Gamma = 2\mu/E$ varies between $\frac{2}{3}$ (incompressible material) and 1 (hyperelastic material). From our assumption of a circular cross section it follows that $I = \pi a^4/4$ and $A = \pi a^2$, where a is the radius of the rod. Therefore, $\sqrt{A/I} = 2/a$, which means that the radius of the rod is fixed to 2 in the scaled variables.

These nine equations form a set of nonlinear, partial differential equations of second order in time and in arclength for nine unknows: force, moment, and director basis vectors. The simple stationary solution is the well-known twisted planar ring [1], that we discuss briefly in the next section. In Secs. IV to VI we shall analyze the dynamics of rods near

this equilibrium configuration following the proposition of Goriely and Tabor in Ref. [1]. In Sec. IV and V we study the cases: (i) $\rho=1$ and $b=0$, (ii) $\rho=1$ and $b\neq0$, (iii) $\rho=\rho(s)$ and $b=0$, and (iv) $\rho=\rho(s)$ and $b\neq0$. Before we do that we briefly review the twisted planar ring solution.

III. PLANAR RING CONFIGURATION

The stationary solutions of Eqs. (19)–(21) are obtained by setting the time derivatives equal to zero in the first two of these equations:

$$\mathbf{F}''-\frac{\rho'(s)}{\rho(s)}\mathbf{F}'=0, \tag{22}$$

$$\mathbf{M}'+\mathbf{d}_3\times\mathbf{F}=0. \tag{23}$$

The only acceptable solution of Eq. (22) is $F=$const [see the original Eq. (8)]. Differentiating Eq. (21) with respect to s and using $\mathbf{d}_i'=\mathbf{k}\times\mathbf{d}_i$ gives

$$\mathbf{M}'=[k_1'+(\Gamma-1)k_2k_3]\mathbf{d}_1+[k_2'-(\Gamma-1)k_1k_3]\mathbf{d}_2+\Gamma k_3'\mathbf{d}_3. \tag{24}$$

Replacing Eq. (24) in Eq. (23) and recalling that $\mathbf{F}=\Sigma f_i\mathbf{d}_i$ gives

$$k_1'+(\Gamma-1)k_2k_3=f_2,$$

$$k_2'-(\Gamma-1)k_1k_3=-f_1, \tag{25}$$

$$k_3'=0.$$

These equations can be solved in terms of Euler angles. Let $\mathbf{e}_i$ be a set of orthonormal Cartesian basis vectors and

$$\mathbf{d}_i=\sum_{j=1}^{3}S_{ij}\,\mathbf{e}_j \tag{26}$$

with

$$S=\begin{pmatrix} \cos\theta\cos\phi\cos\psi-\sin\phi\sin\psi & \cos\theta\cos\phi\sin\psi+\sin\phi\cos\psi & -\cos\phi\sin\theta \\ -\cos\theta\sin\phi\cos\psi-\cos\phi\sin\psi & -\cos\theta\sin\phi\sin\psi+\cos\phi\cos\psi & \sin\phi\sin\theta \\ \sin\theta\cos\psi & \sin\theta\sin\psi & \cos\theta \end{pmatrix} \tag{27}$$

In terms of the Euler angles θ, ϕ, and ψ, Eqs. (25) become

$$\theta''-(\psi')^2\sin\theta\cos\theta+\Gamma\psi'(\phi'+\psi'\cos\theta)\sin\theta$$

$$=-(F_1\cos\psi+F_2\sin\psi)\cos\theta+F_3\sin\theta,$$

$$\psi''\sin\theta+2\psi'\theta'\cos\theta-\Gamma\theta'(\phi'+\psi'\cos\theta)$$

$$=F_1\sin\psi-F_2\cos\psi, \tag{28}$$

$$\psi''\cos\theta=\psi'\theta'\sin\theta-\phi'',$$

where we have defined $\mathbf{F}=\Sigma f_i\mathbf{d}_i=\Sigma F_i\mathbf{e}_i$ and used the relation $\mathbf{k}=\frac{1}{2}\Sigma\mathbf{d}_i\times\mathbf{d}_i'$.

The most simple solution to these equations is

$$\mathbf{F}=\Gamma\gamma\kappa\,\mathbf{e}_3,$$

$$\theta=\pi/2,$$

$$\phi=\gamma s+\pi/2, \tag{29}$$

$$\psi=\kappa s$$

for $0\leq s\leq2\pi/\kappa$. The director basis vectors in the Cartesian basis are given by

$$\mathbf{d}_1=\begin{pmatrix} -\cos\gamma s\sin\kappa s \\ \cos\gamma s\cos\kappa s \\ \sin\gamma s \end{pmatrix}, \quad \mathbf{d}_2=\begin{pmatrix} \sin\gamma s\sin\kappa s \\ -\sin\gamma s\cos\kappa s \\ \cos\gamma s \end{pmatrix},$$

$$\mathbf{d}_3=\begin{pmatrix} \cos\kappa s \\ \sin\kappa s \\ 0 \end{pmatrix} \tag{30}$$

and the central curve is

$$\mathbf{x}(s)=\frac{1}{\kappa}(\sin\kappa s\mathbf{e}_1-\cos\kappa s\mathbf{e}_2). \tag{31}$$

This solution is the famous planar ring configuration. The meaning of the integration constants γ and κ is clear: $R=1/\kappa$ is the radius of the ring and $2\pi\gamma/\kappa$ is the total twist, i.e., the number of turns of the vectors $\mathbf{d}_1$ and $\mathbf{d}_2$ about the tangent vector $\mathbf{d}_3$.

The twist and spin vectors can be readily computed and are given below, together with the expression for the force in the $\mathbf{d}_i$ basis:

$$\mathbf{k}=\kappa\sin\gamma s\,\mathbf{d}_1+\kappa\cos\gamma s\,\mathbf{d}_2+\gamma\,\mathbf{d}_3$$

$$=\gamma\cos\kappa s\,\mathbf{e}_1+\gamma\sin\kappa s\,\mathbf{e}_2+\kappa\,\mathbf{e}_3,$$

$$\mathbf{F}=\Gamma\gamma\kappa(\sin\gamma s\,\mathbf{d}_1+\cos\gamma s\,\mathbf{d}_2)=\Gamma\gamma\kappa\,\mathbf{e}_3, \tag{32}$$

$$\omega=0.$$

We remark that all stationary solutions of the Kirchhoff equations (19)–(21) are independent of b or any fluctuation that might exist in the distribution of mass along the rod. The dynamics, however, does depend on these elements. This means, for instance, that the rod may be driven to different equilibria if immersed in different media or had different mass distribution. We investigate the effects of viscosity and mass distribution in the next sections.

IV. EFFECT OF VISCOSITY IN THE HOMOGENEOUS ROD

As we mentioned in the Introduction, the effects of non-homogeneities in the mass distribution along a rod can be drastically reduced if the Reynolds number of the system is too small. In this section we shall study the effects of viscosity alone in the rod dynamics. Nonuniformities in the mass density will be treated in the next section. Here we shall adopt the analysis proposed by Goriely and Tabor [2] and focus on the time-dependent behavior of homogeneous rods in the vicinity of the planar ring equilibrium.

Goriely and Tabor present in great detail the method of linear analysis of Eqs. (19)–(21). Here we briefly summarize the main steps of the procedure. The basic idea is to expand the director basis (and all dynamical quantities related to the system) in terms of the director basis of the equilibrium position, the *unperturbed basis*.

Let $\mathbf{d}_i^{(0)}$, $i=1,2,3$ be the solution of the stationary Kirchhoff equations for the twisted planar ring, Eq. (30). The perturbed basis $\mathbf{d}_i$ is written as:

$$\mathbf{d}_i=\mathbf{d}_i^{(0)}+\epsilon\mathbf{d}_i^{(1)}+O(\epsilon^2), \quad i=1,2,3, \tag{33}$$

where ϵ is a small parameter. The corrections $\mathbf{d}_i^{(1)}$ are obtained from the Kirchhoff equations and from the requirement that the perturbed basis remains orthonormal to order ϵ, i.e., $\mathbf{d}_i\cdot\mathbf{d}_j=\delta_{ij}+O(\epsilon^2)$. This implies that the vectors $\mathbf{d}_i^{(1)}$ can be written as

$$\mathbf{d}_i^{(1)}=\boldsymbol{\alpha}\times\mathbf{d}_i^{(0)}, \tag{34}$$

where $\boldsymbol{\alpha}$ is a vector to be determined. The perturbed rod can be reconstructed by integrating the tangent vector:

$$\mathbf{x}(s)=\int^s\mathbf{d}_3 ds=\int^s[\mathbf{d}_3^{(0)}+\epsilon(\alpha_2\mathbf{d}_1^{(0)}-\alpha_1\mathbf{d}_2^{(0)})]ds. \tag{35}$$

All dynamical quantities are likewise expanded to first order in the perturbation parameter ϵ. For any such quantity $\mathbf{G}$ we write

$$\mathbf{G}=\mathbf{G}^{(0)}+\epsilon\mathbf{G}^{(1)}+O(\epsilon^2)=(G_i^0+\epsilon G_i^1)\mathbf{d}_i \tag{36}$$

and, in terms of $\mathbf{d}_i^0$,

$$\mathbf{G}^{(0)}=\sum_i g_i^{(0)}\mathbf{d}_i^{(0)}, \tag{37}$$

$$\mathbf{G}^{(1)}=\sum_i[g_i^{(1)}+(\boldsymbol{\alpha}\times\mathbf{G}^{(0)})_i]\mathbf{d}_i^{(0)}. \tag{38}$$

In this section we consider only the case of constant density, $\rho'=0$ and $\rho=1$. Applying this perturbation expansion to the Kirchhoff equations we obtain a system of six equations of second order in s and t for the six independent variables α_1, α_2, $\alpha_3, f_1^{(1)}$, $f_2^{(1)}$, and $f_3^{(1)}$. The form of these equations is not particularly enlightening and, therefore, we shall not write them down. They involve the variables $f_i^{(1)}$, which are the terms $g_i^{(1)}$ of Eq. (38) for $\mathbf{G}=\mathbf{F}$, and $f_i^{(0)}$ and $k_i^{(0)}$, which are the ith component of the force and the twist vector, respectively, in the equilibrium configuration. These equations can be formally written as

$$L_E(\mathbf{k}^{(0)},\mathbf{f}^{(0)})\cdot\boldsymbol{\mu}=0, \tag{39}$$

where $\boldsymbol{\mu}\equiv(\alpha_1,\alpha_2,\alpha_3,f_1^{(1)},f_2^{(1)},f_3^{(1)})$ and L_E is a linear, second-order differential operator in s and t whose coefficients depend on s through the stationary solution $(\mathbf{k}^{(0)},\mathbf{f}^{(0)})$.

For the planar ring solution, the vectors $\mathbf{k}$, $\boldsymbol{\omega}$, and $\mathbf{F}$ are given, in the $\mathbf{d}_i^{(0)}$ basis, by $\mathbf{k}^{(0)}=(\kappa\sin\gamma s,\kappa\cos\gamma s,\gamma)$, $\boldsymbol{\omega}^{(0)}=0$ and $F^{(0)}=(\Gamma\gamma\kappa\sin\gamma s,\Gamma\gamma\kappa\cos\gamma s,0)$, where γ is the twist density, and $\kappa=1/R$ and R is the radius of the rod [see Eq. (32)]. The equations for α_i and f_i can be further simplified with the help of new variables [2]

$$\boldsymbol{\beta}=R_\gamma\cdot\boldsymbol{\alpha} \tag{40}$$

and

$$\mathbf{g}=R_\gamma\cdot\mathbf{f}^{(1)}, \tag{41}$$

where

$$R_\gamma=\begin{pmatrix} \cos\gamma s & -\sin\gamma s & 0 \\ -\sin\gamma s & -\cos\gamma s & 0 \\ 0 & 0 & 1 \end{pmatrix} \tag{42}$$

This transformation leads to an autonomous set of differential equations for $\boldsymbol{\beta}$ and $\mathbf{g}$:

$$\ddot{\beta}_1+b\dot{\beta}_1=g_2'',$$

$$\ddot{\beta}_2+b\dot{\beta}_2+g_1''+2\kappa g_3'-\Gamma\gamma\kappa\beta_3''+2\kappa^2\Gamma\gamma\beta_1'$$
$$=\kappa^2 g_1-\kappa^3\Gamma\gamma\beta_3,$$

$$\Gamma\gamma\kappa\beta_1''+g_3''+2\kappa^2\Gamma\gamma\beta_3'-2\kappa g_1'=\kappa^2 g_3+\kappa^3\Gamma\gamma\beta_1,$$

$$\ddot{\beta}_1+2b\dot{\beta}_1-\beta_1''+\Gamma y\beta_2'-\Gamma\kappa\beta_3'=(1-\Gamma)\kappa^2\beta_1+g_2,$$

$$\ddot{\beta}_2+2b\dot{\beta}_2-\beta_2''-\Gamma\gamma\beta_1'=-g_1+\Gamma\gamma\kappa\beta_3,$$

$$2\ddot{\beta}_3+4b\dot{\beta}_3=\Gamma\beta_3''-\Gamma\kappa\beta_1'. \tag{43}$$

The general form of periodic solutions for $\boldsymbol{\beta}$ and $\mathbf{g}$ can be obtained in terms of a Fourier analysis:

$$\beta_j = e^{\sigma t}(a_j e^{in\kappa s} + \text{c.c.}), \quad j=1,2,3, \tag{44}$$

$$g_j = e^{\sigma t}(a_{j+3} e^{in\kappa s} + \text{c.c.}), \quad j=1,2,3, \tag{45}$$

where c.c. stands for *complex conjugate*, n is an integer that defines the mode of the fundamental solutions, and σ is the characteristic exponent of each mode. Substituting these ex-

pressions into the differential equations for $\boldsymbol{\beta}$ and $\mathbf{g}$ leads to a 6×6 linear system

$$L \cdot a = 0, \tag{46}$$

where

$$L = \begin{pmatrix} 2i\kappa^3\Gamma\gamma n & \sigma^2+b\sigma & \kappa^3\Gamma\gamma(1+n^2) & -\kappa^2(1+n^2) & 0 & 2in\kappa^2 \\ -\sigma^2-b\sigma & 0 & 0 & 0 & -n^2\kappa^2 & 0 \\ -\kappa^3\Gamma\gamma(1+n^2) & 0 & 2i\kappa^3\Gamma\gamma n & -2in\kappa^2 & 0 & -\kappa^2(1+n^2) \\ -\kappa^2(\Gamma+n^2-1)-\sigma^2-2b\sigma & -i\kappa\Gamma\gamma n & i\Gamma\kappa^2 n & 0 & 1 & 0 \\ i\kappa\Gamma\gamma n & -n^2\kappa^2-\sigma^2-2b\sigma & \kappa\Gamma\gamma & -1 & 0 & 0 \\ -i\Gamma\kappa^2 n & 0 & -\Gamma n^2\kappa^2-2\sigma^2+4b\sigma & 0 & 0 & 0 \end{pmatrix}, \tag{47}$$

The eigenvector corresponding to the null eigenvalue determines the coefficients a_j. The imposition that $\Delta \equiv \det L$ is zero determines σ. The determinant can be computed analyically and gives

$$\begin{aligned}
\Delta =& -2\kappa^2(n^4\kappa^2-2n^2\kappa^2+n^2+1+\kappa^2)(n^2\kappa^2+1)\sigma^6 - 2b\kappa^2[6\kappa^4 n^2(-1+n^2)^2+4(1+n^2)+5\kappa^2(1-n^2+2n^4)]\sigma^5 \\
& -\kappa^2\{2b^2[12\kappa^4 n^2(-1+n^2)^2+5(1+n^2)+8\kappa^2(1-n^2+2n^4)]+\kappa^2 n^2(2\Gamma\kappa^4+2n^4\Gamma\kappa^2-2\kappa^4+\Gamma n^2-10n^4\kappa^4+3\Gamma\kappa^2 \\
& -3\Gamma\kappa^4 n^2-4n^2\kappa^2+4n^6\kappa^4+8\kappa^4 n^2+\Gamma+\Gamma n^2\kappa^2+4n^4\kappa^2+\Gamma n^6\kappa^4)\}\sigma^4 - b\kappa^2\{4b^2[1+n^2+4\kappa^4 n^2(-1+n^2)^2 \\
& +\kappa^2(2-2n^2+4n^4)]+\kappa^2 n^2[4\kappa^2(-1+n^2)(2\kappa^2+3n^2-6\kappa^2 n^2+4\kappa^2 n^4)+\Gamma(2+9\kappa^2+8\kappa^4+2n^2+3\kappa^2 n^2-12\kappa^4 n^2 \\
& +6\kappa^2 n^4+4\kappa^4 n^6)]\}\sigma^3 - \kappa^4 n^2\{\kappa^4 n^2(-1+n^2)[2\kappa^2-\Gamma\kappa^2+2\Gamma n^2-4\kappa^2 n^2-\Gamma\kappa^2 n^2+2\kappa^2 n^4+2\Gamma\kappa^2 n^4 \\
& -2\gamma^2\Gamma^2(-1+n^2)]+b^2[8\kappa^2(-1+n^2)(\kappa^2+n^2-3\kappa^2 n^2+2\kappa^2 n^4)+\Gamma(1+6\kappa^2+8\kappa^4+n^2+2\kappa^2 n^2-12\kappa^4 n^2+4\kappa^2 n^4 \\
& +4\kappa^4 n^6)]\}\sigma^2 + 2b\kappa^8 n^4(-1+n^2)[-\Gamma n^2+2\gamma^2\Gamma^2(-1+n^2)-\kappa^2(-1+n^2)(-2+\Gamma+2n^2+2\Gamma n^2)]\sigma \\
& +\Gamma\kappa^{10} n^6(-1+n^2)^2[\gamma^2\Gamma^2-\kappa^2(-1+n^2)]. \tag{48}
\end{aligned}$$

Solutions with real positive σ identify the unstable modes. These are the most relevant modes, since they grow exponentially even for small perturbations. Although the general solution of the equations of motion is a linear combination of these modes, the one with the largest exponent dominates the dynamics and we call it *the principal mode*.

If we set $b=0$ we recover the *dispersion relation* that is presented in Ref. [2]. We see that the viscosity does not change the critical value of the twist Tw for which the stationary solution first becomes unstable. Setting $\sigma=0$ in the above relation we obtain

$$Tw = \frac{\gamma}{\kappa} = \pm\frac{\sqrt{n^2-1}}{\Gamma}, \tag{49}$$

which is independent of b. The lowest mode for which we have an unstable solution is $n=2$ and this leads to Zajac's critical twist: $Tw_c = \sqrt{3}/\Gamma$ [11].

In Fig. 1 we see typical plots of σ versus n for $b=0$, 0.01, and 0.02 with the parameters $\kappa=0.05$, $\gamma=0.375$, and

$\Gamma=0.9$. In all cases we see that the maximum value for σ corresponds to the mode $n=5$. This mode, for the above parameters is, then, the *principal mode*. For large n all modes are damped. Notice that $\sigma(n=5)$ decreases with b. Figure 2 shows on the left the principal mode $n=5$ for $b=0$. In this figure the rod has been slightly moved from its unstable equilibrium position and evolved according to the linearized equations for a (scaled) time $t=130$. For $b\neq 0$, the shape of
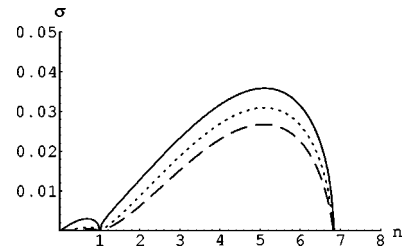

FIG. 1. σ versus n for a homogeneous rod with $b=0$ (full line), $b=0.01$ (dotted line) and $b=0.02$ (dashed line). In all cases $\kappa=0.05$, $\gamma=0.375$, and $\Gamma=0.9$.
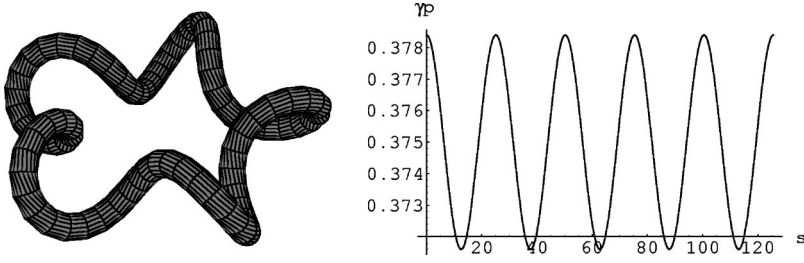
FIG. 2. Left: homogeneous rod with $\kappa = 0.05$, $\gamma = 0.375$, $\Gamma = 0.9$, and $b = 0$ evolved for $t = 130$. Right: twist density $\gamma_p(s)$ for the same rod.

the evolved rod is identical to that shown in this figure for $b = 0$. The only effect of the viscous medium is to slow down the dynamics. At $b = 0.01$, for instance, it takes $t = 150$ to reach the same configuration and for $b = 0.02$ it takes $t = 180$. The shape is symmetric with respect to rotations of $2\pi/5$ about the z axis for all values of b.

The component k_3 of the twist vector is the twist density $\gamma_p(s)$, along the closed rod in the perturbed configuration. The expression for $\gamma_p(s)$ is

$$\gamma_p(s) = \gamma + \epsilon(\alpha_3' + \alpha_2 k_1^{(0)} - \alpha_1 k_2^{(0)}). \qquad (50)$$

Using Eqs. (40), (41), and (42) this can be written as

$$\gamma_p(s) = \gamma + \epsilon(\beta_3' - \kappa\beta_1). \qquad (51)$$

It is interesting to calculate the so-called *linking number Lk* of the perturbed closed rod. The White's formula defines [22,23] the Lk as

$$Lk = Tw + W, \qquad (52)$$

where Tw is the *total twist* of the rod,

$$Tw = \frac{1}{2\pi} \int_0^L k_3(s)ds, \qquad (53)$$

and W is the *writhing number* of a closed space curve. Despite the existence of an explicit formula for the writhing number [22] of any space curve, we calculate it using the White's formula (52) because of the topological invariance of the linking number, i.e., the linking number is a constant for closed rods. Thus, the linking number of the unperturbed configuration (planar ring) is the sum of its total twist and its writhing number. The writhing number of a planar ring is zero [23]:

$$W^{(0)} = 0. \qquad (54)$$

The total twist is calculated using Eq. (53) and for $k_3^{(0)} = \gamma$ and $L = 2\pi/\kappa$. We obtain

$$Tw^{(0)} = \frac{\gamma}{\kappa}. \qquad (55)$$

Then, the linking number is

$$Lk = Tw^{(0)} + W^{(0)} = \frac{\gamma}{\kappa}. \qquad (56)$$

We now can calculate the total twist of the perturbed configuration through the Eq. (51). Since the $\beta_i(s)$ are oscillatory functions of the arclength s [see Eqs. (44) and (45)] the integral in Eq. (53) is null for the term in order $O(\epsilon)$ and the total twist of the perturbed rod is the same of the planar ring:

$$Tw = \frac{1}{2\pi} \int_0^{2\pi/k} \gamma_p(s)ds = \frac{1}{2\pi} \int_0^{2\pi/k} \gamma ds = \frac{\gamma}{\kappa}. \qquad (57)$$

The writhing number of the perturbed rod is

$$W = Lk - Tw = 0. \qquad (58)$$

Therefore, we choose the twist density, as a function of arc length s, as the main quantity to show how each cross section deforms along the closed rod. Figure 2 also shows, on the right, the twist density $\gamma_p(s)$ for the mode $n = 5$.

V. EFFECT OF VISCOSITY IN THE NONHOMOGENEOUS ROD

After having studied how the viscosity affects the near equilibrium dynamics of the twisted planar ring we introduce nonuniformities in the rod, allowing for small variations in the mass density ρ, simulating either fine-scale properties that have survived the large scale limit or the binding of external particles to the filament. For closed rods ρ must be a periodic function of s. Here we consider only the simplest type of periodic dependence, namely,

$$\rho(s) = 1 + \zeta \cos Q\kappa s, \qquad (59)$$

where ζ is the perturbation amplitude ($\zeta \ll 1$) and Q is an integer parameter that fixes the number of complete oscillations of the density along the rod length $L = 2\pi/\kappa = 2\pi R$ [see Eq. (17)] .

We start from Eqs. (19)–(21). Since $\rho(s) \neq 0$, we multiply Eq. (19) by $\rho(s)$:

$$\rho \mathbf{F}'' - \rho b \dot{\mathbf{d}}_3 = \rho'(\mathbf{F}' - b\dot{\mathbf{x}}) + \rho^2 \ddot{\mathbf{d}}_3. \qquad (60)$$

We rewrite the other two Kirchhoff equations for the sake of clarity:

$$\mathbf{M}' + \mathbf{d}_3 \times \mathbf{F} - 2b(\mathbf{d}_1 \times \dot{\mathbf{d}}_1 + \mathbf{d}_2 \times \dot{\mathbf{d}}_2)$$
$$= \rho(s)(\mathbf{d}_1 \times \ddot{\mathbf{d}}_1 + \mathbf{d}_2 \times \ddot{\mathbf{d}}_2), \qquad (61)$$

$$\mathbf{M} = k_1\mathbf{d}_1 + k_2\mathbf{d}_2 + \Gamma k_3\mathbf{d}_3. \qquad (62)$$

Let us first study the case $b=0$. Equations (60) and (61) become

$$\rho \mathbf{F}'' = \rho' \mathbf{F}' + \rho^2 \ddot{\mathbf{d}}_3, \tag{63}$$

$$\mathbf{M}' + \mathbf{d}_3 \times \mathbf{F} = \rho(s)(\mathbf{d}_1 \times \ddot{\mathbf{d}}_1 + \mathbf{d}_2 \times \ddot{\mathbf{d}}_2). \tag{64}$$

Following the same steps of Sec. III we obtain the equations for g_i and β_i for this case

$$\rho^2 \ddot{\beta}_1 - \rho g_2'' + \rho' g_2' = 0,$$

$$\rho^2 \ddot{\beta}_2 + \rho g_1'' + 2\rho \kappa g_3' - \Gamma \gamma \kappa \rho \beta_3'' + 2\kappa^2 \Gamma \gamma \rho \beta_1'$$
$$+ \Gamma \gamma \kappa \rho' \beta_3' - \rho' g_1'$$
$$= \kappa^2 \rho g_1 - \kappa^3 \Gamma \gamma \rho \beta_3 + \Gamma \gamma \kappa^2 \rho' \beta_1 + \kappa \rho' g_3,$$

$$\Gamma \gamma \kappa \rho \beta_1'' + \rho g_3'' + 2\kappa^2 \Gamma \gamma \rho \beta_3' - 2\kappa \rho g_1' - \Gamma \gamma \kappa \rho' \beta_1' - \rho' g_3'$$
$$= \kappa^2 \rho g_3 + \kappa^3 \Gamma \gamma \rho \beta_1 + \Gamma \gamma \kappa^2 \rho' \beta_3 - \kappa \rho' g_1,$$

$$\rho \ddot{\beta}_1 - \beta_1'' + \Gamma y \beta_2' - \Gamma \kappa \beta_3' = (1-\Gamma)\kappa^2 \beta_1 + g_2, \tag{65}$$

$$\rho \ddot{\beta}_2 - \beta_2'' - \Gamma \gamma \beta_1' = -g_1 + \Gamma \gamma \kappa \beta_3,$$

$$2\rho \ddot{\beta}_3 = \Gamma \beta_3'' - \Gamma \kappa \beta_1'.$$

For the case of constant density this constitutes a set of autonomous differential equations for β and g. In the present case these equations are still nonautonomous, since $\rho = \rho(s)$. However, the general form of periodic solutions for β and g can still be obtained as a linear combination of Fourier components:

$$\beta_j = e^{\sigma t} \left(\sum_{n=0}^{\infty} a_{j,n} e^{in\kappa s} + \text{c.c.} \right), \quad j=1,2,3, \tag{66}$$

$$g_j = e^{\sigma t} \left(\sum_{n=0}^{\infty} a_{j+3,n} e^{in\kappa s} + \text{c.c.} \right), \quad j=1,2,3. \tag{67}$$

where c.c. stands for *complex conjugate* and σ is characteristic exponent of the solution. Substituting these expressions

into the differential equations for β and g leads to an infinite dimensional linear system whose matrix is composed of 6×6 blocks labeled by n. Once again, the imposition that the determinant of this matrix is zero determines σ, and the eigenvector corresponding to the null eigenvalue determines the coefficients $a_{j,n}$. If we set the density perturbation parameter ζ to zero, these blocks decouple from each other and the results of Ref. [2] are recovered. For nonzero ζ the block n couples to the blocks $n \pm Q$, $n \pm 2Q$, ..., etc. [see Eqs. (59) and (63)]. Each previously decoupled mode n changes into a new, modified mode. In order to find this new mode n numerically we have considered only the two nearest blocks to n, namely, $n-Q$ and $n+Q$, reducing the system to a set of 18 linear equations. In this approximation all terms in ζ^2 are neglected.

Before we show the numerical results for this case, let us consider the general situation, where $b \neq 0$. In this case, Eq. (60) presents a technical problem, since it has a term proportional to $\dot{\mathbf{x}}$. The vector $\mathbf{x}$ is the space curve of the rod, with the property that $\mathbf{x}' = \mathbf{d}_3$. One possible approach to treat this equation is to differentiate it once more with respect to s and write it entirely in terms of the $\mathbf{d}_i$ vectors. This, however, leads to third-order derivatives of F and introduces spurious solutions that are hard to control. To avoid these complications, we opt for writing Eq. (60) in the fixed Cartesian basis $\{\mathbf{e}_1, \mathbf{e}_2, \mathbf{e}_3\}$. For that, we use the relation between the vectors $\mathbf{d}_i^{(0)}$ and $\mathbf{e}_i$ given by Eqs. (26), (27), and (29).

To calculate $\dot{\mathbf{x}}$ we consider Eq. (35):

$$\mathbf{x}(s) = \int^s \mathbf{d}_3 ds = \int^s [\mathbf{d}_3^{(0)} + \epsilon(\alpha_2 \mathbf{d}_1^{(0)} - \alpha_1 \mathbf{d}_2^{(0)})] ds$$
$$\equiv \mathbf{x}^0(s) + \mathbf{x}^1(s), \tag{68}$$

where α_i is written in terms of β_i using Eq. (40):

$$\alpha_1 = -\beta_2 \cos \gamma s - \beta_1 \sin \gamma s, \tag{69}$$

$$\alpha_2 = \beta_1 \cos \gamma s - \beta_2 \sin \gamma s. \tag{70}$$

Using the series expansion for β and g, Eqs. (66) and (67), we can perform the integral in Eq. (68) explicitly. We obtain the following result for $\mathbf{x}^{(1)}$, considering only the two nearest exponents to n, namely, $n-Q$ and $n+Q$:

$$\mathbf{x}^{(1)}(s) = \frac{e^{\sigma t}}{2} \left\{ -\frac{a_{2,n-Q}}{(n-Q+1)\kappa} e^{i(n-Q+1)\kappa s} + \frac{a_{2,n-Q}}{(n-Q-1)\kappa} e^{i(n-Q-1)\kappa s} - \frac{a_{2,n}}{(n+1)\kappa} e^{i(n+1)\kappa s} + \frac{a_{2,n}}{(n-1)\kappa} e^{i(n-1)\kappa s} \right.$$

$$\left. -\frac{a_{2,n+Q}}{(n+Q+1)\kappa} e^{i(n+Q+1)\kappa s} + \frac{a_{2,n+Q}}{(n+Q-1)\kappa} e^{i(n+Q-1)\kappa s} + \text{c.c.} \right\} \mathbf{e}_1 - \frac{e^{\sigma t}}{2} \left\{ \frac{a_{2,n-Q}}{i(n-Q+1)\kappa} e^{i(n-Q+1)\kappa s} \right.$$

$$+ \frac{a_{2,n-Q}}{i(n-Q-1)\kappa} e^{i(n-Q-1)\kappa s} + \frac{a_{2,n}}{i(n+1)\kappa} e^{i(n+1)\kappa s} + \frac{a_{2,n}}{i(n-1)\kappa} e^{i(n-1)\kappa s} + \frac{a_{2,n+Q}}{i(n+Q+1)\kappa} e^{i(n+Q+1)\kappa s}$$

$$\left. + \frac{a_{2,n+Q}}{i(n+Q-1)\kappa} e^{i(n+Q-1)\kappa s} + \text{c.c.} \right\} \mathbf{e}_2 + e^{\sigma t} \left\{ \frac{a_{1,n-Q}}{i(n-Q)\kappa} e^{i(n+Q)\kappa s} + \frac{a_{1,n}}{in\kappa} e^{in\kappa s} + \frac{a_{1,n+Q}}{i(n+Q)\kappa} e^{i(n+Q)\kappa s} + \text{c.c.} \right\} \mathbf{e}_3.$$

$$\tag{71}$$

Then, $\dot{\mathbf{x}}^{(1)} = \sigma \mathbf{x}^{(1)}$. To write the other terms of Eq. (60) in the $\{\mathbf{e}_1, \mathbf{e}_2, \mathbf{e}_3\}$ basis we define the following quantities:

$$A \equiv \rho^2 \ddot{\beta}_1 + \rho b \dot{\beta}_1 - \rho g_2'' + \rho' g_2', \tag{72}$$

$$B \equiv \rho^2 \ddot{\beta}_2 + \rho b \dot{\beta}_2 + \rho g_1'' + 2\rho\kappa g_3' - \Gamma\gamma\kappa\rho\beta_3'' + 2\kappa^2\Gamma\gamma\rho\beta_1'$$
$$+ \Gamma\gamma\kappa\rho'\beta_3' - \rho' g_1' - \kappa^2\rho g_1 + \kappa^3\Gamma\gamma\rho\beta_3$$
$$- \Gamma\gamma\kappa^2\rho'\beta_1 - \kappa\rho' g_3, \tag{73}$$

$$C \equiv \Gamma\gamma\kappa\rho\beta_1'' + \rho g_3'' + 2\kappa^2\Gamma\gamma\rho\beta_3' - 2\kappa\rho g_1' - \Gamma\gamma\kappa\rho'\beta_1'$$
$$- \rho' g_3' - \kappa^2\rho g_3 - \kappa^3\Gamma\gamma\rho\beta_1 - \Gamma\gamma\kappa^2\rho'\beta_3 + \kappa\rho' g_1. \tag{74}$$

The new three equations for the case $\rho' \neq 0$ and $b \neq 0$ are the three components of the following vector equation:

$$\begin{pmatrix} -B\sin\kappa s + C\cos\kappa s \\ B\cos\kappa s + C\sin\kappa s \\ A \end{pmatrix} = -\sigma\rho' b\mathbf{x}^{(1)}. \tag{75}$$

To complete the set of equations we add the last three of Eqs. (65), modified by the addition of terms proportional to b:

$$\rho\ddot{\beta}_1 + 2b\dot{\beta}_1 - \beta_1'' + \Gamma y\beta_2' - \Gamma\kappa\beta_3' = (1-\Gamma)\kappa^2\beta_1 + g_2,$$

$$\rho\ddot{\beta}_2 + 2b\dot{\beta}_2 - \beta_2'' - \Gamma\gamma\beta_1' = -g_1 + \Gamma\gamma\kappa\beta_3, \tag{76}$$

$$2\rho\ddot{\beta}_3 + 4b\dot{\beta}_2 = \Gamma\beta_3'' - \Gamma\kappa\beta_1'.$$

Since we only consider terms with exponents n, $n-Q$, and $n+Q$ in Eqs. (66) and (67), we again have a system of 18 equations for 18 variables $a_{j,p}$ with $j = 1$ to 6 and $p = n - Q, n, n+Q$.

Figure 3 shows the principal mode $n = 5$ for the parameters $\kappa = 0.05$, $\gamma = 0.375$, $\Gamma = 0.9$, $Q = 1$, and $b = 0$, 0.01, and 0.02. For each value of b we show the effect of nonuniformities in the mass density for $\zeta = 0.03$, 0.07, and 0.10. The time necessary for the unstable rod with $b \neq 0$ to attain the same amplitude as for $b = 0$ with $t = 130$ is obtained through the numerical relation $\sigma t = \sigma(b=0) t(b=0) = 4.7$. As b increases, σ decreases and t, therefore, also increases. In all figures showing rods with nonhomogeneous distribution of mass, we use a grayscale along the rod to indicate the density; black represents places where the density is small, whereas white indicates regions of high density. For $\zeta = 0$ the shape is symmetric with respect to rotations of $2\pi/5$ about the z axis for all values of b as shown in Sec. III. As the density gradient increases the $2\pi/5$ symmetry is broken and the more massive regions of the rod tend to restore the original planar circular shape, decreasing the writhing. Notice that the substantial difference in the shapes of the figures from left to right is caused by a change of just 10% in the local density. Nevertheless, when b becomes much larger than σ, this effect is strongly damped. For $b = 0.05$ (not shown) the effect of the nonuniform density is negligible.
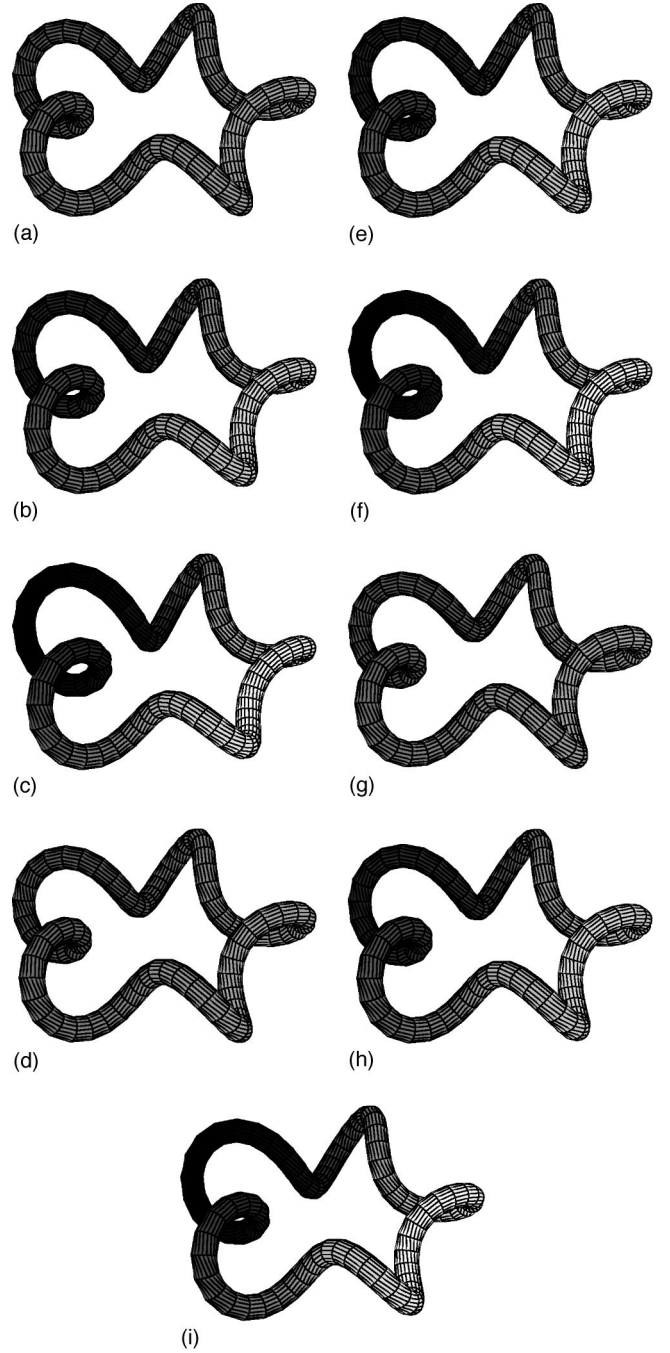

FIG. 3. Principal mode $n = 5$ for a rod with $\kappa = 0.05$, $\gamma = 0.375$, $\Gamma = 0.9$, and $Q = 1$. The viscous coefficient b is 0 for (a)–(c), $b = 0.01$ for (d)–(f), and 0.02 for (g)–(i). For each of these sets of figures the nonuniformity parameter ζ is equal to 0.03, 0.07, and 0.10. The evolution time in each case is $t = 130$ for $b = 0$, $t = 150$ for $b = 0.01$, and $t = 180$ for $b = 0.02$. The grayscale tones indicate the mass gradient along the rod, which is large when white and small when black.

Figure 4 shows the time evolution of the ring with $b = 0$ and $\zeta = 0.1$. It is clear from this figure that, as time passes, the part of ring with lower mass density pops out of the plane and bends while the more massive part stays almost static. In this case, as in Sec. III, the writhing number of these curves is null. Figure 5 shows the plot of the twist density $\gamma_p(s)$
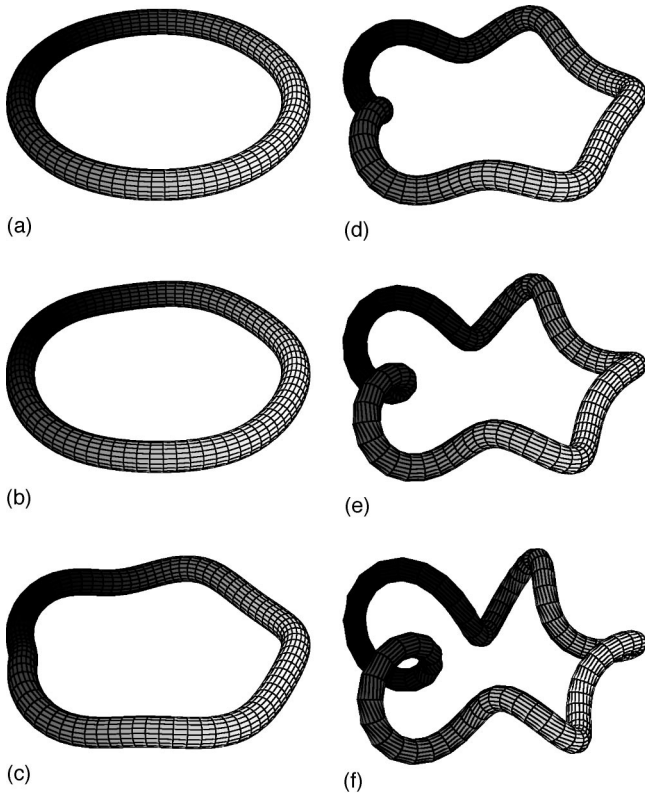
(a)

(b)

(c)

(d)

(e)

(f)

FIG. 4. Time evolution of the principal mode $n=5$ for $\kappa = 0.05$, $\gamma=0.375$, $\Gamma=0.9$, $Q=1$, and $\zeta=0.1$ [see rod in (c)]: (a) $t=0$, (b) $t=40$, (c) $t=80$, (d) $t=105$, (e) $t=120$, and (f) $t=130$. The grayscale tones are the same as in Fig. 3.

versus arclength s for $\zeta=0.1$ and $b=0$, 0.01, and 0.02. In these plots we see the variation of the local twist density with the arclength s. The variation is smaller where the mass density is larger, but this effect decreases as b increases.

Figure 6 shows a rod with $b=0.05$ and $\gamma=0.75$, twice as twisted as before. We see that, now, the symmetry break occurs even at high viscosity, showing that the asymmetric deformation does not depend only on the medium but also on the applied stresses on the rod.

Figure 7 shows a much larger ring, with radius $R=1/\kappa = 200$. Here, $\gamma=0.375$, $\Gamma=0.9$, and $b=0$. In this case the principal mode is $n=50$ and we show the effect of a periodic oscillation of the density with $Q=10$. For the sake of clarity, only the central curve of the rod is drawn. The case $Q=10$ replicates the effect shown in Fig. 3; each high-density segment of the ring tends to a more flat position while the small
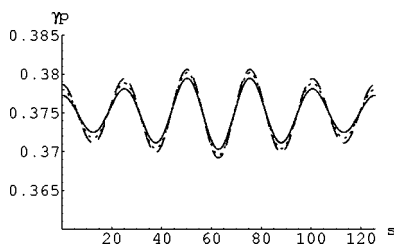

FIG. 5. Twist density $\gamma_p(s)$ for $\zeta=0.1$ and b equal 0, 0.01, and 0.02 (full, dotted, and dashed lines, respectively).
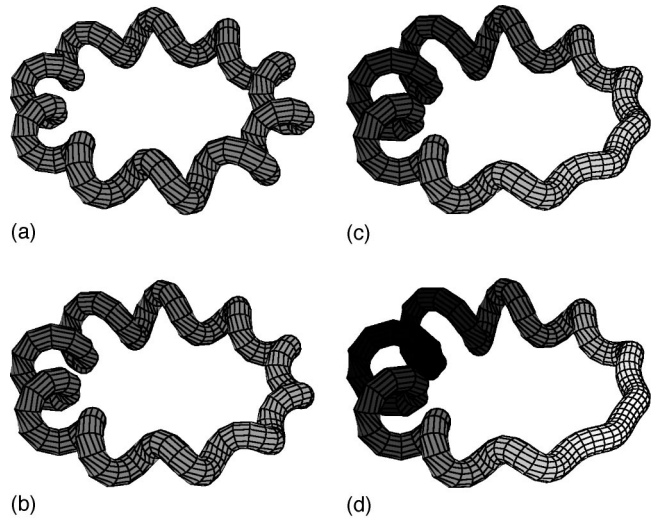

(a)

(b)

(c)

(d)

FIG. 6. Rod twice as twisted as those in previous figures. Here $\kappa=0.05$, $\gamma=0.75$, $Q=1$, $t=45$, and $b=0.05$. The density parameter ζ, from top right to bottom left, is 0, 0.03, 0.07, and 0.10. The inertial effects would be invisible for $\gamma=0.375$.

density parts coil in large loops. Figure 8 shows the effect for $b=0.01$ and $b=0.02$.

We have also considered the case where the frequency of the density oscillations Q, is much higher than the frequency of the last unstable mode, $\sqrt{1+\Gamma\gamma^2/\kappa^2}$. In this case the ring behaves as if the density were constant. This is an interesting result that might be used as a quantitative criterion for neglecting the structural details of the filament and treat it as a uniform rod approach.

VI. APPLICATION TO DNA

In this section, we apply the theory described above to a circular DNA with 168 base pairs (bps) immersed in water.
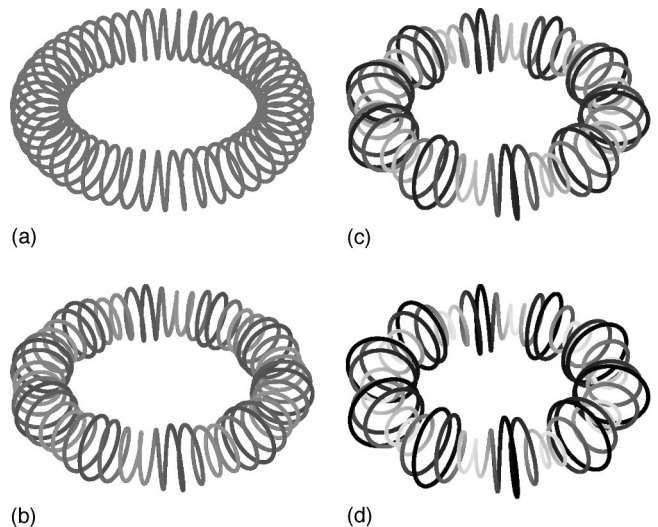

(a)

(b)

(c)

(d)

FIG. 7. Rings ten times larger than those in previous figures. Here $\kappa=0.005$, $\gamma=0.375$, $Q=10$, $t=185$, $b=0$, and ζ, from top right to bottom left, is 0, 0.03, 0.07, and 0.10.
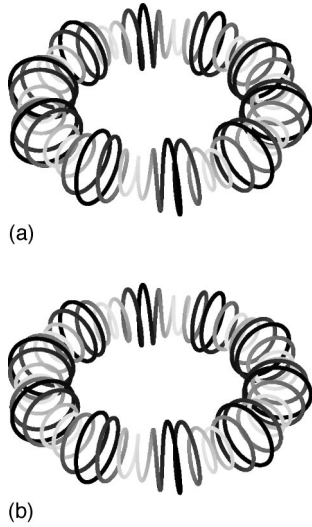
(a)

(b)

FIG. 8. Same as in Fig. 7 with $\zeta=0.1$ and (a) $b=0.01$, $t=215$ and (b) $b=0.02$, $t=250$.

The choice of this system is motivated by a recent experiment by Han *et al.* in short DNA rings [24], where sequences of base pairs with intrinsic bending tendency were synthetized. The rings were immersed in a solution containing Zn^{2+} and/or Mg^{2+}. The authors found that the DNA rings were always stable in a pure Mg^{2+} solution, but exhibited *kinks* above a critical concentration of Zn^{2+} ions (either alone or in combination with Mg^{2+}). This experiment was analyzed theoretically by Haijun and Zhong-can [25] who showed that a possible explanation for these results is that the Zn^{2+} ions enhance the intrinsic curvature of the ring by binding directly to the base pairs, destabilizing the ring. The Mg^{2+} ions, on the other hand, have the opposite effect due to their binding to the phosphate backbone.

Although the instabilities observed in these rings apparently originate from an excess of bending, and not from an excess of twist, we notice that the atomic mass of Zn is of the order of 10% of the total base pair mass (including the phosphates), while that of Mg is only about 4%. Therefore, the binding of Zn^{2+} ions to the DNA provides a neat example of the type of situation our model may describe. In what follows we wish to show that even at low Reynolds number, a sufficiently large stress, like a large twist, can enhance the effects of the inertial forces derived from such a nonhomogeneous distribution of mass.

The Reynolds number for DNA rings in water can be calculated from Eq. (11). The ratio η/ρ_m for water is 10^{-2} cm^2 s^{-1} [18]. The radius of the cross section of the DNA is $a=10$ Å. Assuming an average velocity U for the

DNA of order 0.1 Å s^{-1}, the Reynolds number becomes $R_e=10^{-14}$. Using Eq. (15) we can calculate the constant b and we obtain $b\simeq1.12\times10^{14}$ Nm^{-1} s.

The next step is to apply Eqs. (18) to obtain scaled variables. The scaled κ and b are given by

$$\kappa=\kappa_{esc}\sqrt{\frac{A}{I}}\quad\text{and}\quad b=\sqrt{\frac{AE\rho_0}{I}}b_{esc}.$$

For a DNA of length 168 bps we have $L=168\times l_0$, where $l_0=3.3$ Å is the length of a basepair [26]. Then $\kappa=2\pi/L\simeq113\times10^6$ m^{-1}. Since the ratio

$$\sqrt{\frac{A}{I}}=\sqrt{\frac{\pi a^2}{\pi a^4/4}}=\frac{2}{a}=\frac{1}{5\text{Å}},$$

we find $\kappa_{esc}=0.057$. The mass density of the DNA is $\rho_0=m_{bp}/V_{disc}=929$ kg m^{-3} [26] and the Young's modulus $E=4\times10^8$ Nm^{-2} [14], so that $b_{esc}=0.098$. The dimensionless elastic parameter of the DNA can be taken as $\Gamma=2/3$ [27]. Finally the twist density γ can be calculated from $\gamma_{esc}=Tw\,\kappa_{esc}$.

Most plasmids have linking numbers that are about 5% away from elastic equilibrium [21]. Since the B form of DNA has an approximate twist of 10.5 bps per turn when relaxed, we have $Lk\simeq16$ for the DNA with 168 bps. From Eq. (49) we see that, even for $\Gamma=1$, the minimum value of Tw for which the ring is unstable is $\sqrt{3}\simeq1.73$ for the mode $n=2$. On the other hand, 5% of $Tw=16$ is $0.8<\sqrt{3}$ and, therefore, this DNA minicircle is stable. Indeed, Haijun and Zhong-can [25] showed that the kink deformations observed in this DNA are caused by bending, and not by twisting.

The effects of inertial forces, however, are better visualized on unstable rings. We therefore consider here an artificial excess of linking number equal to 16, corresponding to 100% of the natural twist, and a zero spontaneous curvature. Such a ring does not represent those in the experiment of Ref. [24], but is just inspired by it.

Figure 9 shows on the left the plot of σ versus n for the above parameters. We see that the principal mode is $n=8$. Figure 10 shows the principal mode of the perturbed DNA minicircle for various values of the perturbation amplitude ζ(0, 0.03, 0.07, and 0.1). We see that, despite the very low value of Reynolds number, the effects produced by the inertial forces are the same as in Sec. V. The regions with larger mass density deform less than those with smaller densities. Figure 9 also shows on the right the twist density of
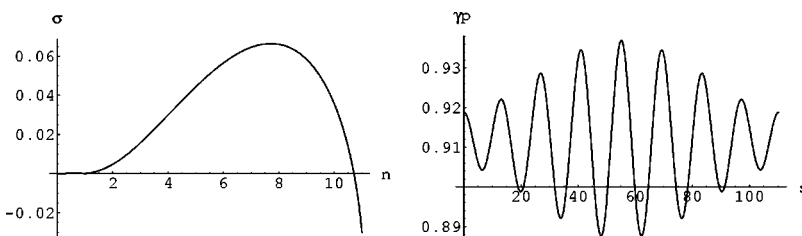

FIG. 9. Right: σ versus n for a DNA ring with $\kappa=0.057$, $\gamma=16\kappa$, and $\Gamma=2/3$. Left: twist density $\gamma_p(s)$ for this ring after a time $t=70$ with $Q=1$, $\zeta=0.1$, and $b=0.098$ (see next figure, bottom right).
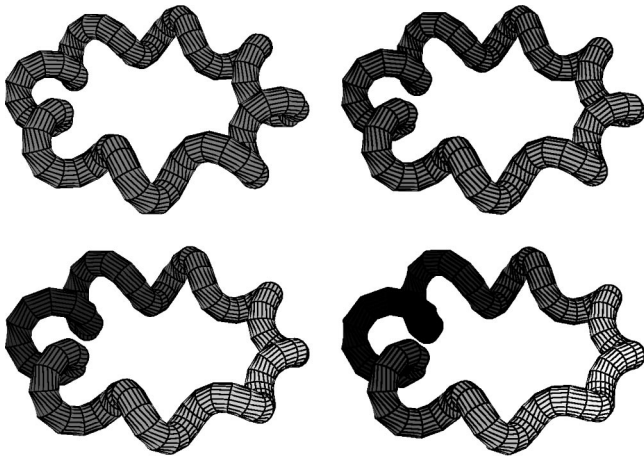
FIG. 10. DNA ring with $b=0.098$ evolved for $t=70$ and mass non-uniformities of 0, 0.03, 0.07, and 0.10.

the perturbed rod $\gamma_p(s)$. Again, the amplitude of variation of $\gamma_p(s)$ is of the same order as in the examples considered in Sec. V.

We finally notice that, although the theory in Ref. [25] does account for the onset of instability of the DNA rings in the experiment of Han *et al.*, it does not explain the asymmetric shapes exhibited by most of the kinked rings shown in Ref. [24]. Our results suggest that this asymmetry is due to nonuniformities in the rings, either intrinsic or induced by the binding of ions.

VII. CONCLUSIONS

The Kirchhoff model of rods is a very powerful framework to study the dynamics of elastic filaments. It allows one to treat a large variety of situations where the rod might be subjected to external forces and nonhomogeneities. In many cases of interest, including biological molecules, the filaments are immersed in a viscous medium with small Reynolds number. In this paper, we start from the general form of the Kirchhoff equations and we incorporate external viscous forces explicitly. In this framework, we have studied the balance between viscosity and the inertial forces induced by a nonhomogeneous distribution of mass along the rod. We showed that the equations determining the equilibrium configurations are independent of both the viscosity and the mass distribution, although the dynamics does usually depend on these elements. Instead of solving the full nonlinear partial equations of the model, we restricted ourselves to the study of the dynamics in the vicinity of the simplest equilibrium configuration of the system, the so-called twisted planar ring. This was done using the method developed by Goriely and Tabor. The results we obtained are summarized below.

The main effect of viscosity on a homogeneous rod, in the vicinity of the planar ring configuration, is to slow down motion. The unstable modes of the near equilibrium dynamics keep the same symmetry for all values of the viscous parameter b studied and the dynamics are almost identical to that without viscosity, only in slow motion.

This effect is also important for rods with varying mass density. In this case, however, the unstable modes of the homogeneous rod problem couple to each other and the shape of the rod changes qualitatively, breaking the symmetry of the individual modes. We observe that the higher-density segments of the rod coil less than the lower-density parts.

The inertial effects generated by the varying mass distribution competes, however, with those of the viscous forces. When the viscous parameter b is larger than the unstable exponent σ the symmetry break is negligible and the rod behaves just like a uniform filament in a very viscous medium. We found, however, that even at very low Reynolds number, a large value of the twist density of the rod tends to enhance the effect of the inertial forces, reviving the coupling between modes and the symmetry breaking. We therefore conclude that *the asymmetric deformations resulting from inertial forces induced by a nonuniform distribution of mass do not depend exclusively on the Reynolds number, but also on the applied stresses on the rod.*

As an interesting example, we applied our model to a DNA minicircle of 168 basepairs (bps) with zero intrinsic curvature and 100% of twisting excess. In DNA molecules, the difference in mass between the basepairs is always less than 0.5%. The DNA, therefore, has an approximate uniform mass density. Nonuniform mass distribution may, however, result from the binding of proteins [14,28,29] or ions [25] to the DNA. Since the interaction of DNA's with these particles are very important in processes like transcription, replication [26], and in the action of the repressors [30], our approach might bring new insights to the dynamics of these processes when the DNA is subjected to large stresses.

In macroscopic systems, like those found in engineering, the Reynolds number is much larger than those found in biological systems. The results described here are then directly applicable with $b \approx 0$. We finally notice that, when the frequency of oscillations in the mass density is larger than the last unstable mode, $n = \sqrt{1 + \Gamma \gamma^2/\kappa^2} \approx \sqrt{\Gamma} \gamma/\kappa$, the rod behaves as if the density was constant.

[1] A. Goriely and M. Tabor, Phys. Rev. Lett. **77**, 3537 (1996).

[2] A. Goriely and M. Tabor, Physica D **105**, 20 (1997); **105**, 45 (1997).

[3] J.P. Keener, J. Fluid Mech. **211**, 629 (1990); S. Da Silva and

A.R. Chouduri, Astron. Astrophys. **272**, 621 (1993).

[4] M.D. Barkley and B.H. Zimm, J. Chem. Phys. **70**, 2991 (1979); Y. Yang, I. Tobias, and W.K. Olson, *ibid.* **98**, 1673 (1993); Y. Shi and J.E. Hearst, *ibid.* **101**, 5186 (1994); J.F.

Marko and E.D. Siggia, Phys. Rev. E **52**, 2912 (1995).

[5] T. Schlick, Curr. Opin. Struct. Biol. **5**, 245 (1995); W.K. Olson, *ibid.* **6**, 242 (1996).

[6] R.E. Goldstein and S.A. Langer, Phys. Rev. Lett. **75**, 1094 (1995);

[7] C.W. Wolgemuth, T.R. Powers, and R.E. Goldstein, Phys. Rev. Lett. **84**, 1623 (2000).

[8] I. Klapper, J. Compute Phys. **125**, 325 (1996).

[9] J. Coyne, IEEE J. Ocean Eng. **15**, 72 (1990).

[10] E.E. Zajac, Bell Syst. Tech. J. **36**, 1129 (1957).

[11] E. E. Zajac, J. Appl. Mech. **29**, 136 (1962).

[12] Y. Sun and J.W. Leonard, Ocean. Eng. **25**, 443 (1997).

[13] M.A. Vaz and M.H. Patel, Appl. Ocean Res. **22**, 45 (2000).

[14] M.M. Gromiha, M.G. Munteanu, I. Simon, and S. Pongor, Biophys. Chem. **69**, 153 (1997).

[15] M.G. Munteanu *et al.*, TIBS **23**, 341 (1998).

[16] R.S. Manning, J.H. Maddocks, and J.D. Kahn, J. Chem. Phys. **105**, 5626 (1996).

[17] E.H. Dill, Arch. Hist. Exact. Sci. **44**, 2 (1992); B.D. Coleman *et al.*, Arch. Ration. Mech. Anal. **121**, 339 (1993).

[18] E.M. Purcell, Am. J. Phys. **45**, 3 (1977).

[19] L. Landau and E. Lifchitz, *Mécanique des Fluides* (Editions Mir, Moscow, 1971).

[20] R. Kh. Zeytounian, *Les Modéles Asymptotiques de la Mécanique des Fluides II*, Lecture Notes in Physics Vol. 276 (Springer-Verlag, Berlin, 1987).

[21] J.F. Marko and E.D. Siggia, Phys. Rev. E **52**, 2912 (1995).

[22] J.H. White, Am. J. Math. **91**, 693 (1969).

[23] F.B. Fuller, Proc. Natl. Acad. Sci. U.S.A. **75**, 3557 (1978).

[24] W. Han, S.M. Lindsay, M. Dlakic, and R.E. Harrington, Nature (London) **386**, 563 (1997); W. Han, M. Dlakic, Y.-J. Zhu, S.M. Lindsay, and R.E. Harrington, Proc. Natl. Acad. Sci. U.S.A. **94**, 10 565 (1997).

[25] Zhou Haijun and Ou-Yang Zhong-can, J. Chem. Phys. **110**, 1247 (1999).

[26] T. Lipniacki, Phys. Rev. E **60**, 7253 (1999).

[27] M.E. Hogan and H. Austin, Nature (London) **329**, 263 (1987).

[28] R.A. Grayling, K. Sandman, and J. Reeve, FEMS Microbiol. Rev. **18**, 203 (1996).

[29] H. Robinson *et al.*, Nature (London) **392**, 202 (1998).

[30] A. Balaeff, L. Mahadevan, and K. Schulten, Phys. Rev. Lett. **83**, 4900 (1999).